Available online at www.sciencedirect.com

ScienceDirect

Mendeleev Commun., 2017, **27**, 595–598

Mendeleev Communications

Supramolecular stereoelectronic effect in hemiketals

Maria V. Panova,*[a] Michael G. Medvedev,*[b] Ivan S. Bushmarinov,[b] Ivan V. Ananyev[b] and Konstantin A. Lyssenko[b]

[a] *N. D. Zelinsky Institute of Organic Chemistry, Russian Academy of Sciences, 119991 Moscow, Russian Federation. E-mail: mariya.13.09@gmail.com*

[b] *A. N. Nesmeyanov Institute of Organoelement Compounds, Russian Academy of Sciences, 119991 Moscow, Russian Federation. E-mail: medvedev.m.g@gmail.com*

DOI: 10.1016/j.mencom.2017.11.019

Hemiketals are important targets for crystal prediction and molecular modeling. The supramolecular stereoelectronic effect (SSE) recently found in carboxylic acid associates occurs in hemiketals: the presence and nature of an H-bond acceptor affect the conformational preference of hemiketals. To provide a structural basis for the multitude of biological roles played by hemiketal-containing structures, it is important to accurately model their spatial and dynamic properties, so the SSE in hemiketals should be explicitly implemented in future force fields.

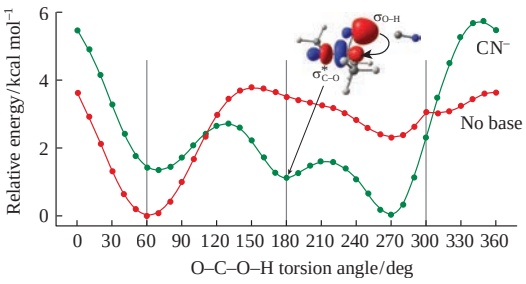

The modeling of intermolecular interactions in organic compounds and biomolecules plays a critical role in various fields of modern chemistry and biochemistry such as crystal prediction,[1,2] molecular docking[3,4] and molecular dynamics.[5,6] To decrease the computational cost of large systems simulations by orders of magnitude, molecular mechanics (MM) methods are used.[7] They are based on the classical laws of atomic motions in predesigned force fields. In molecular modeling, a force field refers to a functional form and parameters set defining molecular system energy from bond lengths, angles and torsion angles between all bonded atoms and from distances between unbonded atoms and molecular fragments. A popular choice of accounting for noncovalent interactions is to limit such interactions to pairwise energies with the Lennard–Jones potential used to consider a van der Waals term and Coulomb's law, for an electrostatic term.[8] Even though noncovalent interactions are considered in this way, in the most common nonpolarizable force fields, it is implied that only bonding interactions can affect torsion energy profiles in molecules. However, as we found earlier,[9] this approximation is fundamentally wrong in some cases. Thus, the formation of a strong hydrogen bond in a carboxylic group leads to a change in its preferred conformation from *cis* to *trans*. Charge redistribution analysis has demonstrated that this effect is closely related to stereoelectronic effects; thus, we proposed the term supramolecular stereoelectronic effect (SSE) for it. Moreover, we have found that the lack of consideration of SSE in common force fields inevitably leads to significant errors in the modeling of crystals and biomolecules, *e.g.*, insulin.

Here, we have studied the strength and importance of SSE in hemiketals, which are commonly found in crystals and biomolecular systems[10] (for example, in carbohydrates) by means of quantum chemical calculations, the subsequent natural bonding orbital (NBO)[11] and atoms-in-molecules (AIM)[12] analyses, and the analyses of crystal structures available in the Cambridge Structural Database (CSD)[13] and Protein Data Bank (PDB).[14] Quantum chemical calculations were performed using Gaussian09[15] program package at the PBE0[16]-D3BJ[17]/cc-pVTZ[18] level of theory. This method was shown to be suitable for organic chemistry calculations[19,20] and well-grounded in theory.[21] NBO, NCI (non-covalent interactions) and AIM analyses were performed at the same level of theory as quantum chemical calculations, using Gaussian09, MultiWFN[22] and AIMAll[23] program packages, respectively.

We used 2-methoxypropan-2-ol as a model structure for quantum chemical calculations (Figure 1). Rotations around the two Me_2C–O bonds in the model hemiketal give rise to five possible nonequivalent conformers. In terms of Me–O–C–O torsion angle, these conformers can be divided into the two groups of *gauche* and *trans* conformers (Figure 1).

For carbohydrates containing hemiacetal or hemiketal fragments, it is commonly assumed that the most stable rotamers are *–gg*, *+gg* and *gt* with the gauche orientation of the OH hydrogen atom.[24]

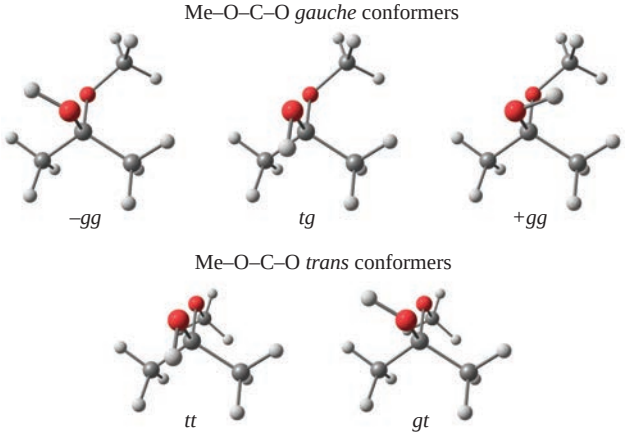

Figure 1 Structures of the nonequivalent conformers of the model hemiketal. The names of conformers are given in terms of rotations around Me_2C–OH (the first symbol) and Me_2C–OMe (the second symbol) bonds. The letters *g* and *t* refer to *gauche* and *trans* substituent orientations, respectively. Plus and minus signs refer to clockwise and anticlockwise hydrogen atom rotations about the OMe group, respectively.

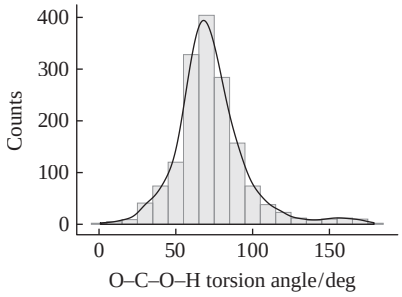

Figure 2 Distribution of O–C–O–H torsion angles (absolute values) for hemiketal fragments in CSD structures.

This is explained by an *exo*-anomeric effect due to overlapping between the σ* orbital of Me_2C–OMe bond and one of the lone pairs of the OH oxygen atom.[25]

However, the analysis of hemiketal-containing structures in CSD has revealed that, in addition to the most frequently encountered structures corresponding to *–gg*, *+gg* and *gt* conformers (the major maximum in Figure 2), there is also a substantial number of *tg* and *tt* conformers corresponding to the minor maximum close to 180°.

Notwithstanding, according to the quantum chemical calculations of the model hemiketal [Figure 3(*a*)], there are no energy minima upon rotation around the Me_2C–OH bond corresponding to *tg* or *tt* conformers. The observed minima correspond to the conformers stabilized *via* the anomeric effect mediated by OH group lone pairs, and they are consistent with earlier reports for similar structures.[26] Thus, the existence of these minima explains the major peak in CSD analysis plot (Figure 2) but not the occurrence of the minor peak corresponding to the O–C–O–H torsion angle near 180°.

However, it should be noted that the hydroxyl groups of hemiketal moieties in CSD structures are almost always hydrogen-bonded to some bases.[27] This fact could explain (in consideration of recently found SSE) the minor peak in Figure 2.

To study the influence of hydrogen bonding on the O–C–O–H torsion angle distribution, we examined it for the model hemiketal containing a hydrogen bond with a strong base CN^- [Figure 3(*b*)]. In this case, we found three minima for both *trans* and *gauche* conformers in contrast with the two minima for the unbonded hemiketal. The new minima correspond to the conformers with an O–C–O–H torsion angle of 180°, which are more energetically favorable than those with an O–C–O–H torsion angle close to 60°. Appearance of these additional minima justifies our hypothesis on the occurrence of SSE in hemiketals.

Note that, in the cyanide-bonded hemiketal, the *+gg* conformer becomes the most favorable due to additional CH···X hydrogen bonding of the anion with the OMe group [weak H-bond in Figure 4(*a*)]. However, the *+gg* conformation of both the model hemiketal and its associate is shifted toward 270° (from an ideal 300° torsion angle) to diminish H–H repulsion interactions of the hydrogen atoms of OH and OMe groups [steric repulsion in Figure 4(*a*)].

Further, we examined the observed SSE effect by means of NBO analysis. Indeed, this effect has a stereoelectronic nature, and it can be explained by interactions between the O–H bonding and Me_2C–OMe anti-bonding NBO orbitals[28] [Figure 4(*b*)]. In the absence of CN^-, their interaction strength is 4.2 kcal mol^{-1}; however, it increases to 5.4 kcal mol^{-1} in the presence of CN^-. Other NBO orbital interactions are not affected that much.

To expand the scope of the found effect, we studied it for the three Me–O–C–O *gauche* conformers of the hemiketal (*–gg*, *tg* and *+gg*, Figure 1) associated with the neutral and anionic bases MeCN, MeCONHMe, CN^-, NCO^- and $MeCOO^-$ (Figure 5). The relative free energy plot indicates that the SSE appears when the hemiketal is associated with anionic rather than neutral bases (this is consistent with the results obtained for carboxylic acids[9]). Importantly, in associates with CN^- and NCO^-, the relative energies of corresponding *tg* conformers are less than 1 kcal mol^{-1}; thus, their contributions to the ensembles should not be neglected. The relatively high energy of the *tg* $MeCOO^-$ associate is due to strong additional hydrogen bonds formed by the carbonyl oxygen of $MeCOO^-$ stabilizing the *–gg* and *+gg* conformers (structures are in Online Supplementary Materials).

The OH···X interaction energy plot shows that the strengths of hydrogen bonds are virtually identical for the three hemiketal

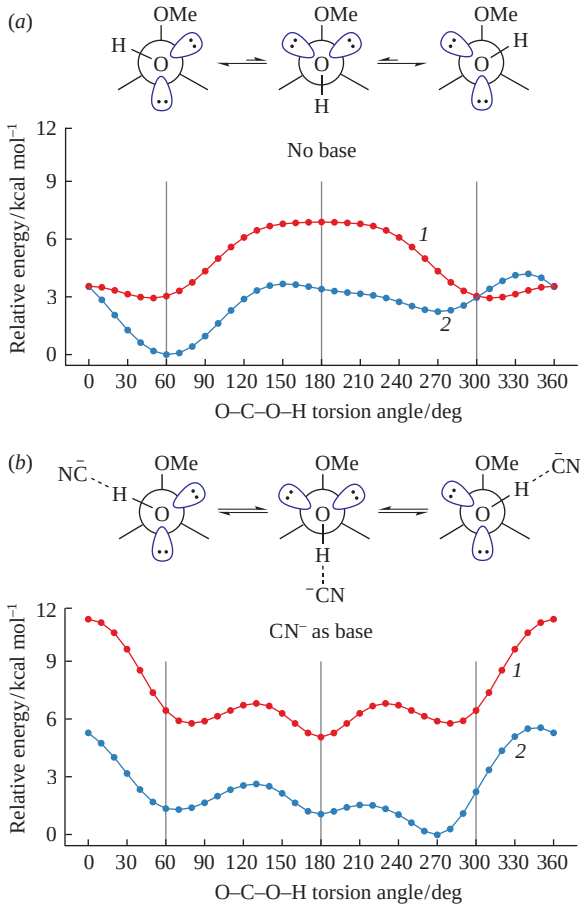

Figure 3 Relative energies of (*a*) the model hemiketal and (*b*) its associate with CN^- in (*1*) *trans* and (*2*) *gauche* Me–O–C–O torsion conformations upon varying the O–C–O–H torsion angle anticlockwise from 0 to 360° in increments of 10°.

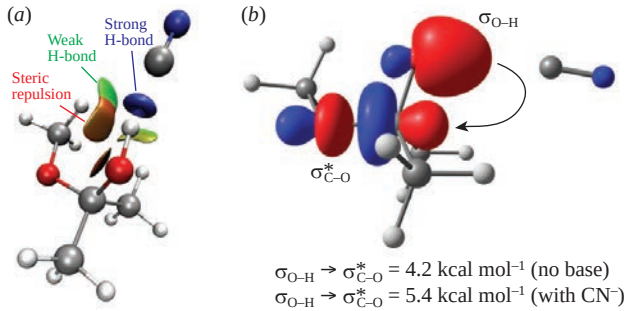

Figure 4 (*a*) NCI analysis of an ideal *+gg* conformer (O–C–O–H torsion angle, 300°) of the model hemiketal bonded to CN^-. Blue-colored isosurface denotes strong H-bond; green-colored, weak H-bonds; red-colored isosurface stands for steric repulsion. (*b*) The NBO analysis of the SSE in the *tg* conformation. The O–H bonding and Me_2C–OMe anti-bonding NBO orbitals, which are responsible for the SSE effect in hemiketals according to the NBO analysis, are shown. In the absence of CN^-, their interaction amounts to 4.2 kcal mol^{-1}, whereas it becomes 5.4 kcal mol^{-1} in the presence of CN^-.

Table 1 Characteristics of the *–gg*, *tg* and *+gg* conformers of the model hemiketal associated with anionic bases (CN^-, NCO^- and $MeCOO^-$).[a]

Base	Conformer	$-V(r)^{OH\cdots X}$	$-V(r)^{CH\cdots X}$ (number of CH···X)	E_{int} (OH···X) / kcal mol^{-1}	E_{int} (CH···X) / kcal mol^{-1}	E_{int} (cumulative) / kcal mol^{-1}
CN$^-$	*–gg*	0.0471	0	14.8	0.0	14.8
	tg	0.0436	0.004 (1)	13.7	1.3	15
	+gg	0.0427	0.0045 (1)	13.4	1.4	14.8
NCO$^-$	*–gg*	0.0624	0.004 (1)	19.6	1.3	20.9
	tg	0.0558	0.0085 (2)	17.5	2.7	20.2
	+gg	0.0546	0.0106 (2)	17.1	3.3	20.4
MeCO**O**$^-$	*–gg*	0.0745	0.0048 (1)	23.4	1.5	24.9
	tg	0.0678	0.0104 (2)	21.3	3.3	24.6
	+gg	0.0736	0	23.1	0.0	23.1

[a] CH···X is an additional hydrogen bond between the H-bonding center and CH hydrogen atoms of hemiketal; $V(r)^{OH\cdots X}$ is potential energy density at the BCP of OH···X interaction; $V(r)^{CH\cdots X}$ is the sum of potential energy densities at the BCPs of the CH···X interactions; E_{int} is interaction energy [estimated from $V(r)$ using the Espinosa–Lecomte–Mollins equation[29]].

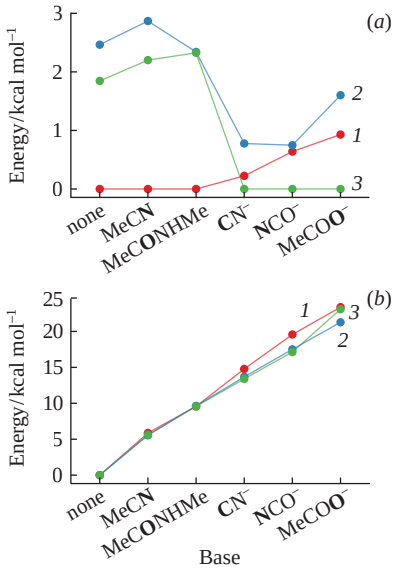

Figure 5 Plots of the (*a*) relative free energies and (*b*) OH···X interaction energies (estimated from the Espinosa–Lecomte–Mollins equation[29]) for the Me–O–C–O *gauche* conformers of the model hemiketal in associates with bases sorted by increasing energy of OH···X interactions: (*1*) *–gg*, (*2*) *tg* and (*3*) *+gg*. The *tg* conformer of the unbonded hemiketal has been obtained by constraining the O–C–O–H torsion angle to 180°. In the case of MeCN associate in *–gg* conformation, we have constrained the OH–N–C angle to 173° to avoid the cleavage of OH···X interaction due to alternative hydrogen bonding.

conformers for a given neutral base. However, for the anionic bases, the strengths of hydrogen bonds are not equal to those of the *–gg* conformer exhibiting the biggest OH···X interaction energies (Figure 5; Table 1). To explain this observation, we performed the AIM analysis of anion-associated hemiketal gauche conformers. In many cases, there are additional hydrogen bonds (CH···X) between the base atom (further, H-bonding center) bonded to the OH group of the hemiketal and the CH hydrogen atoms of hemiketal. Thus, the *tg* and *+gg* conformers usually form one or two CH···X bonds, though the *–gg* conformer has either one or none of them. According to the Espinosa–Lecomte–Mollins equation,[29] the weak interaction energy can be estimated from the potential energy density [$V(r)$, a universal descriptor of interaction strength[30]] at the bond critical point (BCP) of the interaction: $E_{int} = -0.5\,V(r)$. For the *–gg* conformers with the largest OH···X interaction energies, the values of E_{int} corresponding to CH···X interactions are the smallest for a given base (Table 1). Moreover, in the $MeCOO^-$ associate in the *+gg* conformer, the H-bonding center does not form CH···X bonds, and its OH···X interaction energy is very close to that in the *–gg* conformer (Figure 5; Table 1). To summarize these observations, we can conclude that the highest OH···X interaction energies are revealed when there are no CH···X interactions or their relative E_{int} values are small. Note that the sum of the energies of all H···X interactions between the H-bonding center and the hemiketal remains approximately constant for a given base regardless of the number of these interactions (Table 1). A similar effect was recently observed for alkali metal carboxylates with different coordination numbers.[31] We propose a term 'cumulative weak interactions energy permanence' (CWIEP) for this effect. According to it, each weak-bonding center in a given molecule has a constant cumulative weak interactions (CWI) energy. The CWI energies for the studied bases are approximately 15, 20.5 and 24 kcal mol^{-1} for CN^-, NCO^- and $MeCOO^-$, respectively (Table 1).

As noted above, hemiketals are common in both organic crystals and biomolecules, as they are strong bases capable of inducing the supramolecular stereoelectronic effect in them. A survey over the PDB database has demonstrated that SSE takes place in the binding of β-L-ribulose in the D-xylose isomerase active site[32] [PDB ID: 4QE4, Figure 6(*a*)]. Adding hydrogens to the structure with the TSAR[33] algorithm implemented in the Build Model program of the Lead Finder[34] package has revealed that ribulose forms a strong hydrogen bond with the carboxylic group of the Asp287 residue, which stabilizes its *tt* conformation *via* the SSE effect. An analysis of the CSD, in addition to the clear evidence of the SSE in hemiketals (a minor maximum in Figure 2), brought to light a very interesting crystal structure[35] [CSD ID: RIJDOD, Figure 6(*b*)] containing a hemiketal moiety, whose OH group can simultaneously form hydrogen bonds with two ether oxygen atoms with the O–C–O–H torsion angle of 170 or 293° closely corresponding to the ideal *tg* and *+gg* conformations, respectively. However, according to XRD data, the hemiketal occurs only in the *tg* conformation. To exclude experimental errors, we optimized both possible crystal structures (including the unit-cell parameters) in a Γ-point version of the VASP 5.3.4 program package[36] with the PBE[37]-D3[17] functional and a plane-wave basis set (cutoff energy,

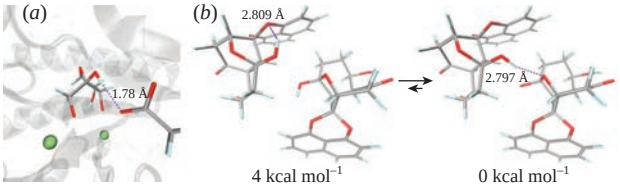

Figure 6 SSE in hemiketal moieties of XRD structures. (*a*) β-L-Ribulose in the active site of the D-xylose isomerase (PDB ID: 4QE4). Positions of hydrogen atoms were calculated with the TSAR[33] algorithm confirmed that the hemiketal moiety occurs in the *tt* conformation. (*b*) Two possible positions of the OH hydrogen in the RIJDOD (CSD ID) crystal. The right structure (bearing *tg* hemiketal moiety) is observed in the crystal and was computed to be 4 kcal mol^{-1} more stable than the left one (with *+gg* hemiketal moiety).

400 eV) with PAW[38] pseudo-potentials. Calculations have revealed that *tg* conformation of the hemiketal moiety is preferred, and its shift to the +*gg* conformer costs 4 kcal mol^{-1} per molecule.

To summarize, we have found that the supramolecular stereoelectronic effect can occur in hemiketals. It stabilizes the *tg* and *tt* conformations (with an O–C–O–H torsion angle close to 180°) of hemiketals bound to strong bases. This effect is clearly visible in the CSD and quantum chemical calculations; its examples can also be found in the PDB database. Since SSE cannot be described with current force fields, it should be explicitly considered in future molecular mechanics methods for crystal prediction and molecular modeling studies involving hemiketal-containing structures. An NBO analysis has demonstrated a stereoelectronic nature of this effect, and showed that it can be explained as interaction between the O–H bonding and Me_2C–OMe antibonding NBO orbitals, which strengthens upon hydrogen bond formation. The AIM analysis of the calculated associates revealed an interesting feature of cumulative weak interactions energy permanence (we denote it as CWIEP), which consists in the invariability of cumulative weak interactions energy (computed according to the Espinosa–Lecomte–Mollins equation) for each weak-bonding center of a given molecule.

M.G.M., I.S.B. and K.A.L. acknowledge the support of the Russian Science Foundation (grant no. 14-13-00884). M.V.P. acknowledges the computational resources provided by the Department of Computational Mathematics and Cybernetics of M. V. Lomonosov Moscow State University (IBM Blue Gene/P supercomputer) and the Federal Center for Collective Usage at 'Kurchatov Institute' (http://computing.kiae.ru/).

Online Supplementary Materials

Supplementary data associated with this article can be found in the online version at doi: 10.1016/j.mencom.2017.11.019.

References

1 S. L. Price, *Chem. Soc. Rev*., 2014, **43**, 2098.
2 A. J. Cruz-Cabeza and J. Bernstein, *Chem. Rev*., 2014, **114**, 2170.
3 N. D. Yilmazer and M. Korth, *Int. J. Mol. Sci*., 2016, **17**, 742.
4 T. V. Pyrkov, I. V. Ozerov, E. D. Balitskaya and R. G. Efremov, *Russ. J. Bioorg. Chem*., 2010, **36**, 446 (*Bioorg. Khim*., 2010, **36**, 482).
5 J. P. Arcon, L. A. Defelipe, C. P. Modenutti, E. D. López, D. Alvarez-Garcia, X. Barril, A. G. Turjanski and M. A. Martí, *J. Chem. Inf. Model.*, 2017, **57**, 846.
6 J. R. Perilla, B. C. Goh, C. K. Cassidy, B. Liu, R. C. Bernardi, T. Rudack, H. Yu, Z. Wu and K. Schulten, *Curr. Opin. Struct. Biol*., 2015, **31**, 64.
7 K. Vanommeslaeghe, O. Guvench and A. D. MacKerell, *Curr. Pharm. Des*., 2014, **20**, 3281.
8 M. Chiu, M. A. Khan and M. C. Herbordt, in *The 19th Annual International IEEE Symposium on Field-Programmable Custom Computing Machines*, IEEE Computer Society, Washington, DC, 2011, pp. 73–76.
9 M. G. Medvedev, I. S. Bushmarinov and K. A. Lyssenko, *Chem. Commun*., 2016, **52**, 6593.
10 V. P. Ananikov, K. I. Galkin, M. P. Egorov, A. M. Sakharov, S. G. Zlotin, E. A. Redina, V. I. Isaeva, L. M. Kustov, M. L. Gening and N. E. Nifantiev, *Mendeleev Commun*., 2016, **26**, 365.
11 A. E. Reed, L. A. Curtiss and F. Weinhold, *Chem. Rev*., 1988, **88**, 899.
12 R. F. W. Bader, *Atoms in Molecules: A Quantum Theory*, Oxford University Press, Oxford, 1994.
13 F. H. Allen, *Acta Crystallogr*., 2002, **B58**, 380.
14 H. M. Berman, J. Westbrook, Z. Feng, G. Gilliland, T. N. Bhat, H. Weissig, I. N. Shindyalov and P. E. Bourne, *Nucleic Acids Res*., 2000, **28**, 235.
15 M. J. Frisch, G. W. Trucks, H. B. Schlegel, G. E. Scuseria, M. A. Robb, J. R. Cheeseman, G. Scalmani, V. Barone, B. Mennucci, G. A. Petersson, H. Nakatsuji, M. Caricato, X. Li, H. P. Hratchian, A. F. Izmaylov, J. Bloino, G. Zheng, J. L. Sonnenberg, M. Hada, M. Ehara, K. Toyota, R. Fukuda, J. Hasegawa, M. Ishida, T. Nakajima, Y. Honda, O. Kitao, H. Nakai, T. Vreven, J. A. Montgomery Jr., J. E. Peralta, F. Ogliaro, M. Bearpark, J. J. Heyd, E. Brothers, K. N. Kudin, V. N. Staroverov, R. Kobayashi, J. Normand, K. Raghavachari, A. Rendell, J. C. Burant, S. S. Iyengar, J. Tomasi, M. Cossi, N. Rega, J. M. Millam, M. Klene, J. E. Knox, J. B. Cross, V. Bakken, C. Adamo, J. Jaramillo, R. Gomperts, R. E. Stratmann, O. Yazyev, A. J. Austin, R. Cammi, C. Pomelli, J. W. Ochterski, R. L. Martin, K. Morokuma, V. G. Zakrzewski, G. A. Voth, P. Salvador, J. J. Dannenberg, S. Dapprich, A. D. Daniels, Ö. Farkas, J. B. Foresman, J. V. Ortiz, J. Cioslowski and D. J. Fox, *Gaussian 09, Revision D.01*, Wallingford, CT, 2009.
16 C. Adamo and V. Barone, *J. Chem. Phys*., 1999, **110**, 6158.
17 S. Grimme, J. Antony, S. Ehrlich and H. Krieg, *J. Chem. Phys*., 2010, **132**, 154104.
18 T. H. Dunning, Jr., *J. Chem. Phys*., 1989, **90**, 1007.
19 R. Peverati and D. G. Truhlar, *Philos. Trans. R. Soc. London, Ser. A*, 2014, **372**, 20120476.
20 N. Mardirossian and M. Head-Gordon, *Mol. Phys*., 2017, **115**, 2315.
21 M. G. Medvedev, I. S. Bushmarinov, J. Sun, J. P. Perdew and K. A. Lyssenko, *Science*, 2017, **355**, 49.
22 T. Lu and F. Chen, *J. Comput. Chem*., 2012, **33**, 580.
23 T. A. Keith, *AIMA II,Version 16.01.09*, TK Gristmill Software, Overland Park, KS, USA, 2015.
24 D. Solís, N. V. Bovin, A. P. Davis, J. Jiménez-Barbero, A. Romero, R. Roy, K. Smetana, Jr. and H.-J. Gabius, *Biochim. Biophys. Acta*, 2015, **1850**, 186.
25 I. V. Alabugin, *Stereoelectronic Effects: A Bridge between Structure and Reactivity*, John Wiley & Sons, Ltd., 2016, ch. 1.
26 G. A. Kasaei, D. Nori-Shargh, H. Yahyaei, S. N. Mousavi and E. Pourdavoodi, *Mol. Simul*., 2012, **38**, 1022.
27 A. Gavezzotti and G. Filippini, in *Computational Approaches in Supramolecular Chemistry*, ed. G. Wipff, Springer, Dordrecht, 1994, pp. 51–62.
28 I. V. Alabugin and T. A. Zeidan, *J. Am. Chem. Soc*., 2002, **124**, 3175.
29 E. Espinosa and E. Molins, *J. Chem. Phys*., 2000, **113**, 5686.
30 I. V. Ananyev, V. A. Karnoukhova, A. O. Dmitrienko and K. A. Lyssenko, *J. Phys. Chem. A*, 2017, **121**, 4517.
31 I. V. Ananyev, I. S. Bushmarinov, I. E. Ushakov, A. I. Aitkulova and K. A. Lyssenko, *RSC Adv*., 2015, **5**, 97495.
32 P. Langan, A. K. Sangha, T. Wymore, J. M. Parks, Z. K. Yang, B. L. Hanson, Z. Fisher, S. A. Mason, M. P. Blakeley, V. T. Forsyth, J. P. Glusker, H. L. Carrell, J. C. Smith, D. A. Keen, D. E. Graham and A. Kovalevsky, *Structure*, 2014, **22**, 1287.
33 O. V. Stroganov, F. N. Novikov, A. A. Zeifman, V. S. Stroylov and G. G. Chilov, *Proteins*, 2011, **79**, 2693.
34 O. V. Stroganov, F. N. Novikov, V. S. Stroylov, V. Kulkov and G. G. Chilov, *J. Chem. Inf. Model*., 2008, **48**, 2371.
35 K. Krohn, K. Beckmann, U. Flörke, H.-J. Aust, S. Draeger, B. Schulz, S. Busemann and G. Bringmann, *Tetrahedron*, 1997, **53**, 3101.
36 G. Kresse and J. Furthmüller, *Comput. Mater. Sci*., 1996, **6**, 15.
37 J. P. Perdew, K. Burke and M. Ernzerhof, *Phys. Rev. Lett*., 1996, **77**, 3865.
38 G. Kresse and D. Joubert, *Phys. Rev. B*, 1999, **59**, 1758.

Received: 26th July 2017; Com. 17/5318